Proceedings of Meetings on Acoustics

Volume 19, 2013 http://acousticalsociety.org/

ICA 2013 Montreal
Montreal, Canada
2 - 7 June 2013

Engineering Acoustics
Session 3aEA: Computational Methods in Transducer Design, Modeling, Simulation, and Optimization II

3aEA4. Design of resonant frequencies for piezoelectric actuator with integrated components

Jun Kuroda*, Yasuharu Onishi, Motoyoshi Komoda, Yasuhiro Oikawa and Yoshio Yamasaki

***Corresponding author's address: Common Platform Development Division, NEC CASIO Mobile Communications, Ltd, Kawasaki, 211-8666, Kanagawa prefecture, Japan, j-kuroda@bq.jp.nec.com**

Piezoelectric actuators are used in a wide range of electrical devices, including piezoelectric speakers, buzzers, haptics and ultrasonic transducers. For piezoelectric actuator systems used in mobile devices, the most important issue is improving the electromechanical conversion efficiency. The power consumed by the actuators must be minimized due to the small size of the batteries used. The frequency response around the mechanical resonance must be carefully designed to enable low power driving. The resonant frequencies of piezoelectric actuators that consist of integrated components, such as the metal cones in ultrasonic speakers, are determined by the energy dispersion of the total system. Therefore, factors such as the size and physical properties of each component must be designed to optimize the resonant frequencies for practical applications. The total energy of the piezoelectric system is described by Lagrange-Maxwell equations. Even though it is not easy to solve the differential equations written in a Lagrangian coordinate system by using exact calculations, useful information for designing systems can be derived from approximate calculations. In this paper, we will introduce design guidelines that can be used to optimize the resonant frequencies of piezoelectric actuators with integrated components, based on analysis using the Lagrangian coordinate system.

Published by the Acoustical Society of America through the American Institute of Physics

 [DOI: 10.1121/1.4799923]
Received 22 Jan 2013; published 2 Jun 2013

INTRODUCTION

Recent portable electronics systems include vibration and acoustic devices for various applications such as haptics and speakers. The vibration devices and drive systems included in portable electronics systems must be small and have an efficient electro-mechanical conversion rate. Piezoelectric actuators have a highly efficiency electro-mechanical conversion rate and are thin and small. Piezoelectric actuators are therefore one solution to achieving the high vibration and acoustic performance required for slim portable devices.[1-5] In some piezoelectric actuator applications, the first and second resonant frequencies must be controlled to obtain the maximum vibration displacement or velocity. However, there are no known simple analytical guidelines to designing resonant frequencies. A piezoelectric actuator consists of several components. The vibration characteristics of the whole actuator are determined by the total energy. However, the coupled energy generated by the components complicates the calculation of the vibration of the whole actuator. In practical design processes, engineers utilize numerical calculation methods, such as the finite element method (FEM), boundary element method (BEM) and finite-difference time-domain method (FDTD), even though these methods cannot provide clear guidelines for streamlining the design. For electro-mechanical transducers, engineers use the Lagrange-Maxwell equation, which provides a rationale for electro-mechanical conversion. The Lagrange-Maxwell equation is equivalent to the partial differential equation used for piezoelectric material and integrated components and contains information about the elasto-piezo-dielectric matrix (EPD matrix) of piezoelectric material and the mechanical properties of the integrated components. It is possible to derive a Lagrange-Maxwell equation that implies all physical information as metric tensors in a Lagrange coordinate system, Nevertheless, the obtained equation cannot be solved easily. To make use of this equation in practical design, it must be simplified by using an algebraic approach. It is empirically known that the vibration of a continuum behaves as if the mechanical mass, stiffness and friction loss were lumped in a low frequency band. Lumped constant approximation is a useful approach, but it must be appropriately employed, carefully considering the mathematical model of the mechanical system.

In this paper, we derive a simple guideline for designing low-order resonant frequencies for piezoelectric actuators and show design examples.

MATHEMATICAL MODELING

In this chapter, the physical model used to derive the mathematical formulas is shown. An ultrasonic speaker with a radiation cone is used as an example of a simple piezoelectric actuator. By considering the characteristics of an ultrasonic speaker, we can obtain the outline of a mathematical model and assume approximate differential equations.

Example of Simple Piezoelectric Actuator

Figure 1 shows the ultrasonic speaker with a radiation cone used as an example of a piezoelectric actuator with integrated components. This type of ultrasonic speaker has been well studied in prior research.[6] This ultrasonic speaker consists of a diaphragm and a cone. The diaphragm is a unimorph-type piezoelectric actuator that consists of a piezoelectric board and a metal board pasted together by a thin adhesive layer (thinner than 10 μm). The radiation cone is required to boost the excluded volume of the air. The diaphragm and the cone are linked by a binder. The cone is made of metal to provide the appropriate stiffness and mass to enable mechanical resonance in an ultrasonic frequency band. The binder is made of an elastic material, such as acrylic resin, PET, ABS resin, or silicon rubber.

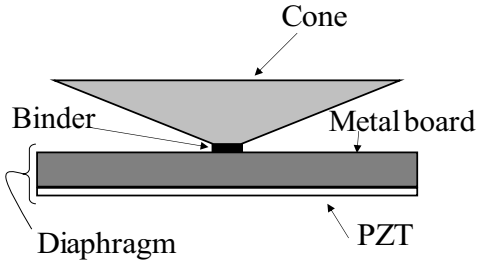

Figure 1. Ultrasonic speaker with radiation cone.

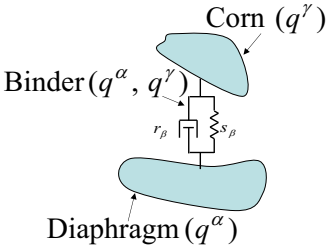

Figure 2. Abstracted mathematical for piezoelectric actuator.

Considering the physical properties of this actuator, the following conditions can be presumed for the mathematical model:

A. The binder is represented by the stiffness and the friction loss connected parallel to each other.
B. The mechanical potential and friction loss of the binder are determined by the sum of the relative distance and velocity between the diaphragm and the cone.
C. The differential equations of the diaphragm and the cone are not changed by the binder connection.
D. The mechanical properties (stiffness, mass density and friction loss) are uniform for all components.

All assumptions above are based on the fact that the binder is much lighter and softer than the diaphragm and the cone, that is, that the diaphragm and the cone behave as rigid bodies against the binder because the material of binder is resin.

Mathematical Modeling and Analytical Formulization for the Example Actuator

Mathematical Modeling

According to assumptions A, B, C and D, the diaphragm and the cone can be abstracted as manifolds. As written above, the detailed shape, dimensions and physical properties can be abstracted in a Lagrange's equation as metric tensors. Each component is named as follows: diaphragm = α, binder = β, and cone = γ. The general Lagrange coordinates are defined as follows:

$$\text{Diaphragm } \alpha : q^{\alpha(i)}, \dot{q}^{\alpha(i)},\ \text{Pillar } \beta : q^{\beta(i)}, \dot{q}^{\beta(i)},\ \text{Binder } \gamma : q^{\gamma(i)}, \dot{q}^{\gamma(i)}.$$
$$\left(\alpha(i),\ \beta(i),\ \gamma(i) \subseteq \mathbf{N}, \alpha(i) \neq \beta(i),\ \beta(i) \neq \gamma(i),\ \gamma(i) \neq \beta(i)\right)$$

This general coordinate system is defined by the arrayed coordinates for all micro areas in a rectangular system, without distinguishing each micro area. Note that $\alpha(i)$, $\beta(i)$, $\gamma(i)$ does not include identical numbers because a unique number is assigned to each micro area. Figure 2 shows the abstracted mathematical model of the piezoelectric actuator.

The total Lagrangian, potential, kinetic energy and energy dissipation are defined as the sum of these values for each component, as follows:

$$L = L^{(\alpha)} + L^{(\beta)} + L^{(\gamma)},\ T = T^{(\alpha)} + T^{(\beta)} + T^{(\gamma)},\ U = U^{(\alpha)} + U^{(\beta)} + U^{(\gamma)},\ J = J^{(\alpha)} + J^{(\beta)} + J^{(\gamma)}, \quad (1)$$

where L is the Lagrangian, T the kinetic energy, U the potential and J the energy dissipation.

The Lagrangian is defined by the potential, the kinetic energy and the Lagrange multiplier term as shown below:

$$L = T - U + \sum_{\mu} \lambda_{\mu} f^{\mu}, \quad (2)$$

where λ_{μ} is the Lagrange multiplier, f^{μ} the restriction condition $\left(\mu \subseteq \mathbf{N}\right)$.

Note that in this paper, the Lagrange multiplier term is used to represent the restriction of the displacement by the binder β. This is described in detail later.

Formularization of the Lagrangian by Metric Tensors

First, we denote the kinetic energy, potential and dissipation in a uniform area by using metric tensors.[7-9] By using the Einstein summation convention, the kinetic energy and the energy dissipation for a rectangular coordinate system are written as follows:

$$T^k = \frac{1}{2} M_{kk} \left\{ (\dot{x}^k)^2 + (\dot{y}^k)^2 + (\dot{z}^k)^2 \right\},\ J^k = \frac{1}{2} R_{kk} \left\{ (\dot{x}^k)^2 + (\dot{y}^k)^2 + (\dot{z}^k)^2 \right\}, \quad (3), (4)$$

where x, y, z are the coordinates for the k-th micro area, M_{kk} the mass of the micro area, R_{kk} the friction loss of the micro area, k the suffix for the micro areas, N number of micro areas $\left(k, N \subseteq \mathbf{N}\right)$.

For rectangular coordinate systems, according to transformation rule of contravariant vectors can be applied to the coordinates as follow:

$$x^k = \frac{\partial x^k}{\partial q^i} q^i, y^k = \frac{\partial y^k}{\partial q^i} q^i, z^k = \frac{\partial x^k}{\partial q^i} q^i, \dot{x}^k = \frac{\partial x^k}{\partial q^i} \dot{q}^i, \dot{y}^k = \frac{\partial y^k}{\partial q^i} \dot{q}^i, \dot{z}^k = \frac{\partial x^k}{\partial q^i} \dot{q}^i \ . \tag{5), (6)}$$

Substituting Eq. (5) and (6) into Eq. (3) and (4), the result is:

$$T^k = \frac{1}{2} M_{kk} \left(\frac{\partial x^k}{\partial q^i} \frac{\partial x^k}{\partial q^j} + \frac{\partial y^k}{\partial q^i} \frac{\partial y^k}{\partial q^j} + \frac{\partial z^k}{\partial q^i} \frac{\partial z^k}{\partial q^j} \right) \dot{q}^i \dot{q}^j = \frac{1}{2} m_{ij} \dot{q}^i \dot{q}^j \ , \tag{7}$$

$$J^k = \frac{1}{2} R_{kk} \left(\frac{\partial x^k}{\partial q^i} \frac{\partial x^k}{\partial q^j} + \frac{\partial y^k}{\partial q^i} \frac{\partial y^k}{\partial q^j} + \frac{\partial z^k}{\partial q^i} \frac{\partial z^k}{\partial q^j} \right) \dot{q}^i \dot{q}^j = \frac{1}{2} r_{ij} \dot{q}^i \dot{q}^j \ . \tag{8}$$

Equation (7) and (8) show that the kinetic energy and the dissipation of the micro areas can be expressed by the metric tensors m_{ij} and r_{ij}, which represent the mass and friction loss. The potential must be derived taking into consideration the variation of the displacement between two micro areas. In the rectangular coordinate system in this paper, the arbitrary point $P:(x,\ y,\ z) = \left(x^1, x^2,\ x^3\right)$, and the micro line element around this point $\left(dx^1,\ dx^2,\ dx^3\right)$ are taken into consideration. When point P moves to $\overline{P}:\left(\bar{x}^1,\ \bar{x}^2,\ \bar{x}^3\right)$, it is assumed that the micro line element becomes $\left(d\bar{x}^1,\ d\bar{x}^2,\ d\bar{x}^3\right)$. Terms higher than the second order can be ignored because this deformation is small enough. The tensor of the distortion is expressed as follows:

$$\epsilon_{ij} \quad = \quad (d\bar{s})^2 - (ds)^2 = d\bar{x}^i d\bar{x}^i - dx^i dx^i = \frac{1}{2}\left(\frac{\partial u^i}{\partial x^j} + \frac{\partial u^j}{\partial x^i} + \frac{\partial u^k}{\partial x^i} \frac{\partial u^k}{\partial x^j} \right) = \frac{1}{2}\left(\frac{\partial u^i}{\partial x^j} + \frac{\partial u^j}{\partial x^i} \right) , \tag{9}$$

where u^j is the variation of the coordinates between points P and $\overline{P}$, defined as $u^k = \bar{x}^k - x^k$.

$$U^k = \frac{1}{2} \epsilon_{kl} dx^k dx^l = \frac{1}{2} \epsilon_{kl} \frac{\partial x^k}{\partial q^i} q^i \cdot \frac{\partial x^l}{\partial q^j} q^j = \frac{1}{2} s_{ij} q^i q^j \ . \tag{10}$$

According to Eq. (7), (8) and (10), the kinetic energy, the energy dissipation and the potential, for the micro areas, could be expressed by the metric tensors. The Lagrangian for whole system is obtained by substituting Eq. (7) and (10) to Eq. (2) and integrating it. The dissipation force is considered separately as it can not be included in the Lagrangian.

Formularization of Lagrange's Equation for the Actuator

The Lagrange's equation for the i-th micro areas including the dissipation is shown below,

$$\frac{d}{dt}\left(\frac{\partial L}{\partial \dot{q}^i} \right) - \frac{\partial L}{\partial q^i} + \frac{\partial J}{\partial \dot{q}^i} = f^i \ . \tag{11}$$

where f is the driving force generated by the electro-distortion of the piezoelectric material.

Considering the electro-distortion in detail, Eq. (11) can be regarded as the Lagrange-Maxwell equation. Lagrange's equations for diaphragm α and cone γ are derived, by using Eq. (2), (7), (8) and (10) and adding the restriction and additional dissipation created by the binder β.

In this paper, we apply the following detailed policy concerning the restriction and dissipation created by binder β to formulize the concrete Lagrange's equations taking into consideration the assumptions of the mathematical models A, B, C and D:

(i) The restriction and energy dissipation created by binder β does not affect the kinetic energy, potential and energy dissipation of diaphragm α and cone γ.

(ii) The restriction and energy dissipation created by binder β is represented by the Lagrange multiplier and additional friction loss, which is added to Equation (14). The Lagrange multiplier terms and the additional dissipation are determined relative to the displacement and the velocity, respectively, of diaphragm α and cone γ. Therefore, the Lagrange multiplier terms and the additional dissipation of diaphragm α and those of cone γ have opposite signs to each other.

By substituting Eq. (2), (7), (8) and (10) into (11) and regarding metric tensors m_{ij}, s_{ij}, r_{ij} as uniform constants m_α, s_α, r_α for diaphragm α and m_γ, s_γ, r_γ for cone γ, denoting the diaphragm and the cone can be derived as shown below;

$$m_\alpha \ddot{q}^{\alpha(i)} + r_\alpha \dot{q}^{\alpha(i)} + s_\alpha q^{\alpha(i)} + \frac{\partial}{\partial q^{\alpha(i)}}\left[\lambda_{\alpha(i)\gamma(i)} f^{\alpha(i)\gamma(i)}\left(q^{\alpha(i)}, q^{\gamma(i)}\right)\right] + \frac{\partial}{\partial \dot{q}^{\alpha(i)}}\left[\kappa_{\alpha(i)\gamma(i)} g^{\alpha(i)\gamma(i)}\left(\dot{q}^{\alpha(i)}, \dot{q}^{\gamma(i)}\right)\right] = F^{\alpha(i)}, \tag{12}$$

$$m_\gamma \ddot{q}^{\gamma(i)} + r_\gamma \dot{q}^{\gamma(i)} + s_\gamma q^{\gamma(i)} - \frac{\partial}{\partial q^{\gamma(i)}}\left[\lambda_{\alpha(i)\gamma(i)} f^{\alpha(i)\gamma(i)}\left(q^{\alpha(i)}, q^{\gamma(i)}\right)\right] - \frac{\partial}{\partial \dot{q}^{\gamma(i)}}\left[\kappa_{\alpha(i)\gamma(i)} g^{\alpha(i)\gamma(i)}\left(\dot{q}^{\alpha(i)}, \dot{q}^{\gamma(i)}\right)\right] = 0, \tag{13}$$

where $\lambda_{\alpha(i)\gamma(i)} f^{\alpha(i)\gamma(i)}$ and $\kappa_{\alpha(i)\gamma(i)} g^{\alpha(i)\gamma(i)}$ represent the Lagrange multiplier term for the displacement and the energy dissipation determined by the velocity.

Equations (12) and (13) includes the equations of the same number of $\alpha(i)$ or $\gamma(i)$, respectively. The term on right-hand side of Eq. (12) and (13) represents the driving force. In Eq. (12), $F^{\alpha(i)}$ is the driving force of the piezoelectric material. In Eq. (13), the term on the right-hand side is zero as there is no driving force for the cone.

By distinguishing the micro areas and expressing $\mathbf{x}^k = \left(x^k, y^k, z^k\right) = \left(q^{k_1}, q^{k_2}, q^{k_3}\right)$ as follows,

$$m_\alpha \ddot{\boldsymbol{x}}^{\alpha(k)} + r_\alpha \dot{\boldsymbol{x}}^{\alpha(k)} + s_\alpha \boldsymbol{x}^{\alpha(k)} + \frac{\partial}{\partial \boldsymbol{x}^{\alpha(k)}}\left[\boldsymbol{\lambda}_{\alpha(k)\gamma(k)} \boldsymbol{f}^{\alpha(k)\gamma(k)}\left(\boldsymbol{x}^{\alpha(k)}, \boldsymbol{x}^{\gamma(k)}\right)\right] + \frac{\partial}{\partial \dot{\boldsymbol{x}}^{\alpha(k)}}\left[\boldsymbol{\kappa}_{\alpha(k)\gamma(k)} \boldsymbol{g}^{\alpha(k)\gamma(k)}\left(\dot{\boldsymbol{x}}^{\alpha(k)}, \dot{\boldsymbol{x}}^{\gamma(k)}\right)\right] = \boldsymbol{F}^{\alpha(k)}, \tag{14}$$

$$m_\gamma \ddot{\boldsymbol{x}}^{\gamma(k)} + r_\gamma \dot{\boldsymbol{x}}^{\gamma(k)} + s_\gamma \boldsymbol{x}^{\gamma(k)} - \frac{\partial}{\partial \boldsymbol{x}^{\gamma(k)}}\left[\boldsymbol{\lambda}_{\alpha(k)\gamma(k)} \boldsymbol{f}^{\alpha(k)\gamma(k)}\left(\boldsymbol{x}^{\alpha(k)}, \boldsymbol{x}^{\gamma(k)}\right)\right] - \frac{\partial}{\partial \dot{\boldsymbol{x}}^{\gamma(k)}}\left[\boldsymbol{\kappa}_{\alpha(k)\gamma(k)} \boldsymbol{g}^{\alpha(k)\gamma(k)}\left(\dot{\boldsymbol{x}}^{\alpha(k)}, \dot{\boldsymbol{x}}^{\gamma(k)}\right)\right] = \boldsymbol{0}, \tag{15}$$

where $\frac{\partial}{\partial \mathbf{x}}$ means $\left(\frac{\partial}{\partial x}, \frac{\partial}{\partial y}, \frac{\partial}{\partial z}\right)$, the Lagrange multiplier terms can be expressed as vectors.

According to the assumption B of the mathematical model, the Lagrange multiplier terms and additional dissipation by the binder can be simplified by performing the integration covering each component. We will omit a rigorous mathematical discussion concerning the simplification of these terms and consider them intuitively by using the assumption B of this mathematical model. Equations (14) and (15) are used to perform integration covering each component (which means totaling all micro areas) as follows:

$$m_\alpha \ddot{\boldsymbol{X}}^{\alpha} + r_\alpha \dot{\boldsymbol{X}}^{\alpha} + s_\alpha \boldsymbol{X}^{\alpha} + s_\beta\left[\boldsymbol{X}^{\alpha} - \boldsymbol{X}^{\gamma}\right] + r_\beta\left[\dot{\boldsymbol{X}}^{\alpha} - \dot{\boldsymbol{X}}^{\gamma}\right] = \boldsymbol{G}^{\alpha}, \tag{16}$$

$$m_\gamma \ddot{\boldsymbol{X}}^{\gamma} + r_\gamma \dot{\boldsymbol{X}}^{\gamma} + s_\gamma \boldsymbol{X}^{\gamma} - s_\beta\left[\boldsymbol{X}^{\alpha} - \boldsymbol{X}^{\gamma}\right] - r_\beta\left[\dot{\boldsymbol{X}}^{\alpha} - \dot{\boldsymbol{X}}^{\gamma}\right] = \boldsymbol{0}, \tag{17}$$

where s_β is the stiffness of the binder, r_β the friction loss of the binder, and $\mathbf{X}^{\alpha} = \sum_{\alpha(i)} \mathbf{x}^{\alpha(i)}$, $\mathbf{X}^{\gamma} = \sum_{\gamma(i)} \mathbf{x}^{\gamma(i)}$.

Equations (16) and (17) are the simultaneous differential equations to be employed in the actual design. Equation (16) and (17) are regard as the electrical equivalent circuit shown in Fig. 3, concerning vector component in each direction. The branch of s_β and r_β combine the energies of the diaphragm and the cone. This simplification can be allowed under the condition that the binder satisfies the assumption A, B, C and D, as written above.

Actuators with many components (Fig. 4) can be described by several pairs of Eq. (18) and (19), which are generalized Eq. (16) and (17) as follows,

$$\begin{cases} m_1 \ddot{\boldsymbol{X}}^{1} + r_1 \dot{\boldsymbol{X}}^{1} + s_1 \boldsymbol{X}^{1} + s_2\left[\boldsymbol{X}^{3} - \boldsymbol{X}^{1}\right] + r_2\left[\dot{\boldsymbol{X}}^{3} - \dot{\boldsymbol{X}}^{1}\right] = \boldsymbol{G}^{1}, & (18) \\ m_3 \ddot{\boldsymbol{X}}^{3} + r_3 \dot{\boldsymbol{X}}^{3} + s_3 \boldsymbol{X}^{3} - s_2\left[\boldsymbol{X}^{3} - \boldsymbol{X}^{1}\right] - r_2\left[\dot{\boldsymbol{X}}^{3} - \dot{\boldsymbol{X}}^{1}\right] = \boldsymbol{G}^{3}, & (19) \end{cases}$$

$$\begin{cases} m_3 \ddot{\boldsymbol{X}}^{3} + r_3 \dot{\boldsymbol{X}}^{3} + s_3 \boldsymbol{X}^{3} + s_4\left[\boldsymbol{X}^{5} - \boldsymbol{X}^{3}\right] + r_4\left[\dot{\boldsymbol{X}}^{5} - \dot{\boldsymbol{X}}^{3}\right] = \boldsymbol{G}^{3}, & (20) \\ m_5 \ddot{\boldsymbol{X}}^{5} + r_5 \dot{\boldsymbol{X}}^{5} + s_5 \boldsymbol{X}^{5} - s_4\left[\boldsymbol{X}^{5} - \boldsymbol{X}^{3}\right] - r_4\left[\dot{\boldsymbol{X}}^{5} - \dot{\boldsymbol{X}}^{3}\right] = \boldsymbol{G}^{5}, & (21) \end{cases}$$

where the driving force $\mathbf{G}^i$ is the electro-distortion generated by the piezoelectric material or other type of electro-magnetic forces.

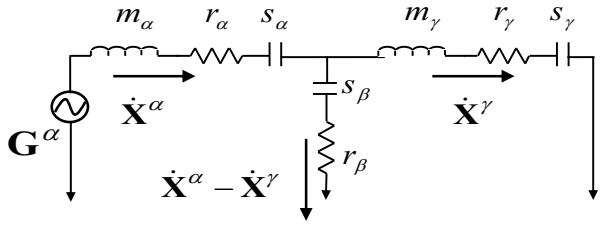

Figure 3. Equivalent circuit for piezoelectric actuator.

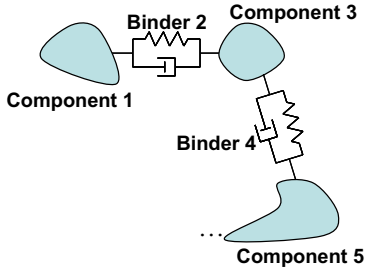

Figure 4. Piezoelectric actuator with three components.

The mass, the stiffness and the friction loss in Eq. (17) and (18) are calculated by integrating of the solution of the differential equation of each component. As long as the differential equation of each component can be solved, Eq. (17) and (18) can be analytically solved and lower order resonant frequencies can be designed.

DESIGNING THE RESONANT FREQUENCIES OF THE ACTUATOR

Above, we determined the mathematical model and formulization for the ultrasonic speaker shown in Fig. 1. In this section, we will show the actual design of the resonant frequencies of a piezoelectric actuator. It has been confirmed that Eq. (16) and (17) can be utilized in the design of resonant frequencies by comparing these with results of numerical calculations.

The formula used to design the resonant frequencies of the actuator can be derived from Eq. (16) and (17). The ideal resonant frequencies, which are the design purpose, are determined according to the relationship between the mass, the stiffness and the friction loss of diaphragm α and cone γ, and are expressed by a simple formula derived from Eq. (16) and (17).

Ultrasonic speakers such as the one shown in Fig. 1 are used to emit an ultrasonic frequency whose center is a lower order-resonant frequency. The power spectrum of the driving voltage input to the speakers spreads around this center frequency. Figure 5 shows the electrical conductance of the ultrasonic speaker AT40-10PB (made by Nippon Ceramic Co., Ltd) and the expected bandwidth of the driving voltage of the single sideband (SSB) signal.[10]

As shown in Fig. 5, an ultrasonic speaker should have a broad peak at the resonant frequencies. However, from the point of view of the mechanical efficiency of the actuator, the mechanical Q factor should not be reduced by the damping. The solution for this issue is to minimize the gap between the first and second resonant frequencies of the piezoelectric actuator.

According to the Fourier transform of the normal component to the diaphragm of Eq. (16) and (17), as the matrix form as follows:

$$\begin{bmatrix} a & b \\ b & c \end{bmatrix} \begin{bmatrix} X^{\alpha} \\ X^{\gamma} \end{bmatrix} = O\,, \tag{22}$$

where the elements of the matrix are

$$a = -m_{\alpha}\omega^2 + i\omega r_{\alpha} + s_{\alpha} + i\omega r_{\beta} + s_{\beta},\ b = -\left(i\omega r_{\beta} + s_{\beta}\right),\ c = -m_{\gamma}\omega^2 + i\omega r_{\gamma} + s_{\gamma} + i\omega r_{\beta} + s_{\beta}\,,$$

and ω is the angular frequency.

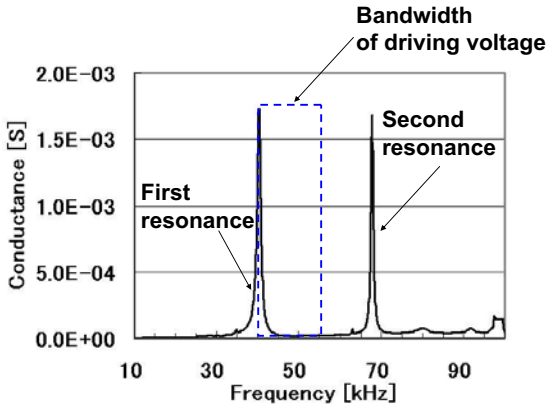

Figure 5. Electrical conductance(AT40-10PB) and bandwidth of driving voltage.

The characteristic equation is expressed as follows:

$$\begin{aligned} &m_{\alpha}m_{\gamma}(\omega^2)^2 - \left\{-r_{\alpha}r_{\beta} - r_{\beta}r_{\gamma} - r_{\gamma}r_{\alpha} - m_{\alpha}s_{\gamma} - m_{\gamma}s_{\alpha} - m_{\gamma}s_{\beta}\right\}\omega^2 + s_{\alpha}s_{\beta} + s_{\beta}s_{\gamma} + s_{\gamma}s_{\alpha} \\ &+ i\left[\left\{-m_{\gamma}r_{\beta} - m_{\alpha}r_{\beta} - m_{\gamma}r_{\alpha} - m_{\alpha}r_{\gamma}\right\}\omega^2 + s_{\alpha}r_{\beta} + s_{\alpha}r_{\gamma} + s_{\beta}r_{\gamma} + s_{\beta}r_{\alpha} + s_{\gamma}r_{\beta}\right] = 0\,. \end{aligned} \tag{23}$$

The positive solution of Eq. (23) is as follows,

$$\omega_1 = \frac{\sqrt{-P_3\sqrt{P_2} + P_3 P_1}}{\sqrt{2}P_3}\,,\quad \omega_2 = \frac{\sqrt{P_3\sqrt{P_2} + P_3 P_1}}{\sqrt{2}P_3}\,, \tag{24}$$

where P_1, P_2 and P_3 are

$$P_1 = r_{\beta}r_{\gamma} + r_{\alpha}r_{\gamma} + r_{\alpha}r_{\beta} + m_{\alpha}s_{\beta} + m_{\alpha}s_{\gamma} + s_{\beta}m_{\gamma} + s_{\alpha}m_{\gamma}\,,$$

$$
\begin{aligned}
P_2 &= -2m_\alpha s_\gamma s_\beta m_\gamma - 2m_\alpha s_\gamma s_\alpha m_\gamma + 2r_\alpha r_\beta m_\alpha s_\beta + 2r_\alpha r_\beta m_\alpha s_\gamma + 2r_\alpha r_\beta s_\beta m_\gamma \\
&+ 2r_\alpha r_\beta s_\alpha m_\gamma - 2m_\alpha s_\beta s_\alpha m_\gamma + 2r_\beta r_\gamma m_\alpha s_\beta + 2r_\beta r_\gamma m_\alpha s_\gamma + 2r_\beta r_\gamma s_\beta m_\gamma + 2r_\beta r_\gamma s_\alpha m_\gamma \\
&+ 2r_\alpha r_\gamma m_\alpha s_\beta + 2r_\alpha r_\gamma m_\alpha s_\gamma + 2r_\alpha r_\gamma s\beta m_\gamma + 2r_\alpha r_\gamma s_\alpha m_\gamma + 2r_\beta{}^2 r_\gamma r_\alpha + 2m_\alpha s_\beta{}^2 m_\gamma \\
&+ 2r_\alpha{}^2 r_\gamma r_\beta + 2m_\alpha{}^2 s_\beta s_\gamma + 2s_\beta m_\gamma{}^2 s_\alpha + 2r_\beta r_\gamma{}^2 r_\alpha + r_\alpha{}^2 r_\beta{}^2 + m_\alpha{}^2 s_\beta{}^2 + m_\alpha{}^2 s_\gamma{}^2 \\
&+ s_\beta{}^2 m_\gamma{}^2 + s_\alpha{}^2 m_\gamma{}^2 + r_\beta{}^2 r_\gamma{}^2 + r_\alpha{}^2 r_\gamma{}^2 , \\
P_3 &= m_\alpha m_\gamma .
\end{aligned}
$$

Two positive solutions ω_1 and ω_2 in Eq. (24) represent the two resonant angular frequencies of the piezoelectric actuator. The purpose of this design is to find the condition of physical properties that minimizes the ratio of ω_1 and ω_2. The optimum mass of the cone m_γ is calculated when all other physical properties have been determined.

The optimum condition of m_γ is derived from the solution of the equation as follows:

$$
\frac{\partial}{\partial m_\gamma}\left[\frac{\omega_1}{\omega_2}\right] = 0 , \quad \frac{\partial^2}{\partial m_\gamma^2}\left[\frac{\omega_1}{\omega_2}\right] > 0 . \tag{25}
$$

The solution of Eq. (25) is calculated as,

$$
m_\gamma = \frac{r_\beta r_\gamma + r_\alpha r_\gamma + r_\alpha r_\beta + m_\alpha s_\beta + m_\alpha s_\gamma}{s_\beta + s_\alpha} . \tag{26}
$$

Equation (26) is the formula used to minimize the gap between the two resonant frequencies.

In Eq. (26), all friction losses are negligible, because metal has a high mechanical Q factor and the amount of the PET is much smaller than metal. The piezoelectric material does not contribute to the resonant frequencies due to its thinness (thinner than 100μm). The piezoelectric material operates simply as just the driving force in Eq. (16) and (17). Figure 6 shows an outline of the piezoelectric actuator used in the design trial. The diaphragm and the cone are disk shaped and they have no restrictions except binder β. Table.1 shows the physical properties of each component used for design calculated by using Eq. (26) and numerical calculation. The material of cone γ is defined as a virtual metal, which has a variable mass density. The optimum design to minimize the frequency gap can be founded by the observing of the variation of the first and second resonant frequencies determined by the mass density of cone ρ_γ.

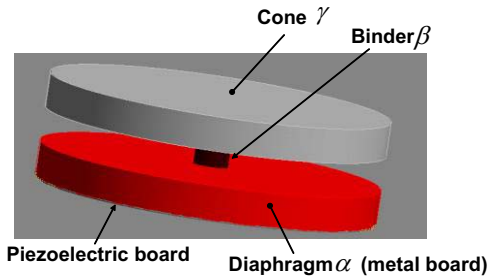

Figure 6. Piezoelectric actuator for design trial.

TABLE 1. Physical properties of components in piezoelectric actuators.

Component	Material	Mass density [kg/m^3]	Young modulus [GPa]	Shape and dimensions
Diaphragm (metal board) α	Phosphor bronze	8.80×10^3	120	Disc shaped, diameter: 1 cm, Thickness: 1 mm
Binder β	PET	1.36×10^3	3.44	Cylinder, diameter: 1 mm, Thickness: 1 mm
Cone γ	Virtual metal	Variable ($5.40\times10^3 - 9.40\times10^3$)	100	Disc shaped, diameter: 1 cm, Thickness: 1 mm

The partial differential equation (PDE) of the bending plate is expressed as follows,

$$\left(\nabla^2\right)^2 \xi = -\frac{q}{D}\frac{\partial^2}{\partial t^2}\xi\,, \tag{27}$$

where ∇^2 is the Laplacian operator, D the bending stiffness, q the driving force and ξ the vibration displacement. Equation (27) can be used for disks with a free edge. The fundamental resonant frequency without a nodal diameter is expressed as below,

$$f_{01} = \frac{0.412h}{a^2}\sqrt{\frac{E}{(1-\sigma^2)}}\,, \tag{28}$$

where a is the diameter of the disk, the h thickness, E the Young modulus, σ the Poisson's ratio.

The mass of each component can be calculated easily and the stiffness can be determined by the relationship; $f = 1/2\pi \cdot \sqrt{k/m}$. The optimum mass density of the cone is calculated as 7400 kg/m^3 by using Eq. (26), (27) and Table.1. For the diaphragm and the cone, the equation is,

$$m_\alpha = \pi a_\alpha^2 \rho = 6.91^{-4}, \quad m_\gamma = \pi a_\gamma^2 \rho = 7.85^{-8}\rho_\gamma\,,$$

$$f_{01_\alpha} = \frac{0.412h_\alpha}{a_\alpha^2}\sqrt{\frac{E_\alpha}{\rho_\alpha(1-\sigma_\alpha^2)}} = 6.38\times10^4, \quad f_{01_\gamma} = \frac{0.412h_\gamma}{a_\gamma^2}\sqrt{\frac{E_\gamma}{\rho_\gamma(1-\sigma_\gamma^2)}} = 5.48\times10^6\sqrt{\frac{1}{\rho_\gamma}}\,,$$

$$s_\alpha = 4\pi^2 f_{01_\alpha}^2 m_\alpha = 1.11\times10^8, \quad s_\gamma = 4\pi^2 f_{01_\gamma}^2 m_\gamma = 9.25\times10^7\,. \tag{29}$$

And for the binder, the equation is,

$$s_\beta = \frac{E_\beta S_\beta}{h_\beta} = 2.70\times10^6\,, \tag{30}$$

where S_β is the area of the cross section, and h_β the height of the binder.

Accordingly, the optimum mass density of the cone is calculated by the following equation as,

$$\pi a_\gamma^2 \rho_\gamma = \frac{m_\alpha s_\beta + m_\alpha s_\gamma}{s_\beta + s_\alpha}\,, \quad \rightarrow \quad \rho_\gamma = 7.36\times10^3\,. \tag{31}$$

To verify this design, the electrical conductance was calculated by FEM simulation using Femtet (made by Murata Software Co., Ltd.), are shown in Fig. 7.

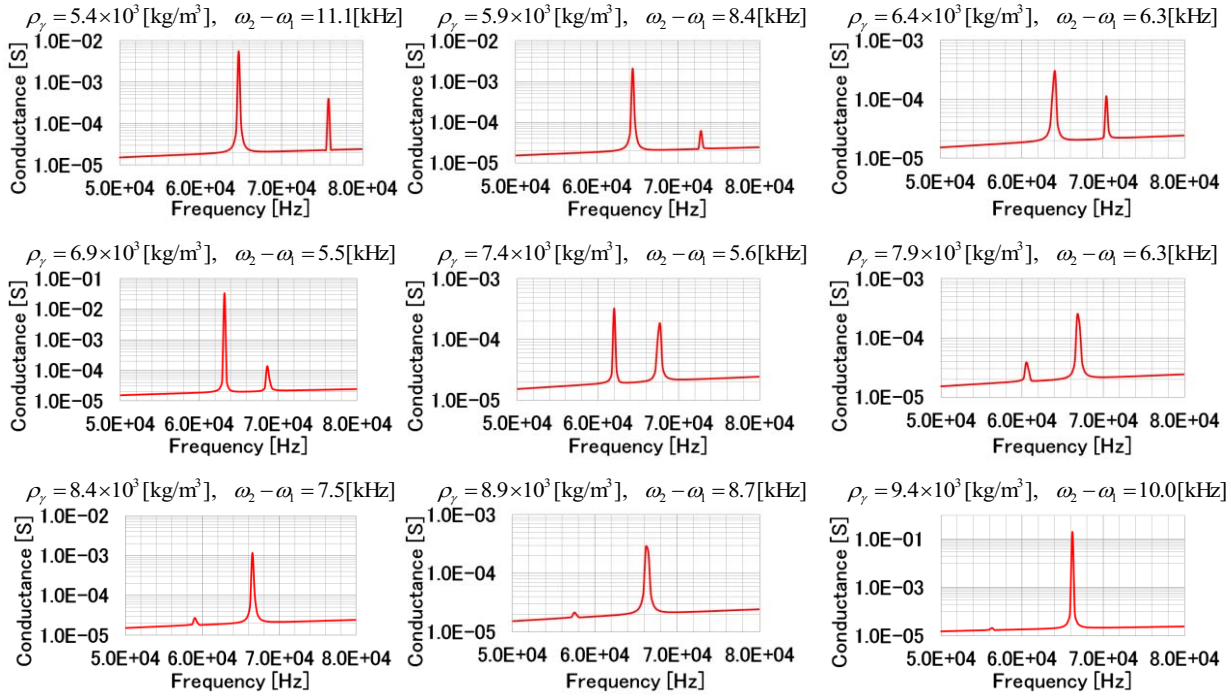

Figure 7. Results of simulating electrical conductance of piezoelectric actuator.

As shown in Fig. 7, the frequency gap is minimized when the mass density ρ_γ is $6.9\times10^3 - 7.4\times10^3$
We could confirm that Eq. (16) and (17) can be used to design the resonant frequencies of the piezoelectric actuators.

CONCLUSIONS

In this paper, we provided a guideline for designing the resonant frequencies of piezoelectric actuators. Piezoelectric actuators consist of several components and have a complex vibration form and mechanical resonance. The components in a piezoelectric actuator form a complex electro-mechanical system with coupled energy, which makes it difficult to design the required characteristics. Therefore, an analytical design approach is necessary to streamline the design process of the actuators. An analytical design approach is, generally, based on solving the partial differential equations (PDEs) and ordinary differential equations (ODEs) of the whole system of the actuator. However, it is almost impossible to solve the PDEs and ODEs of the whole system due to the system's mathematical complexity. To create a practical guideline for designing an actuator, we contrived to detach the energy of each component by using the Lagrangian coordinate system and Lagrange's equation. Derived PDEs with lumped constants have a simple form and can be easily used in actual design. As an example of a design purpose, we showed how we researched the optimum value of the mass of the cone of an ultrasonic speaker to minimize the frequency gap between the first and second resonances. We could confirm that the conclusion of our analytical design accords with the simulation results obtained from FEM.

The proposed approach is useful not only for conventional actuators, but also for new actuators that have complex mechanical links or use electro-magnetic force. Small and highly efficient electro-mechanical and electro-acoustic transducers are in high demand in the portable device market. A mathematical design approach for actuators is therefore important to aid in the development of innovative small and efficient actuators.

REFERENCES

1. T. Ikeda , "Fundamentals of Piezoelectricity," *Oxford Sci-ence Publications, Oxford, New York, Tokyo* (1996).
2. S. Takahashi and S. Hirose , "Vibration-level characteristics of lead zirconate titanate ceramics," *Jpn. J. Appl. Phys.*, 31, pp. 3055–3057 (1992).
3. S. Takahashi, S. Hirose, and K. Uchino, "Stability of PZT piezoelectric ceramics under vibration level change," *J. Am. Ceram. Soc.*, 77, pp. 2429–2432 (1993).
4. S. Takahashi, S. Hirose, K. Uchino, and K. Y. Oh, "Electro-mechanical characteristics of lead zirconate ti-tanate ceramics under vibration-level change," *Proceeding of the 9th IEEE Int'l Symp. Appl Ferroelectrics.*,pp. 377–382 (1994).
5. Jun Kuroda, Yasuhiro Onishi, Motoyoshi Komoda, Yasuhiro Oikawa and Yoshio Yamasaki, "The driving system for piezoelectric speaker with low power consumption," Acoust.Sci.&Tech., Vol.33, No.6, pp.372-375, (2012).
6. S. Sakai, Y. Shiozawa and T. Toi, "Clarification of sound radiation mechanism for airborne ultrasonic transducer," Acoust.Sci.&Tech., Vol.30, No.6, pp.404-409, (2009).
7. T. Sekimoto "Denki Onkyo Henkan Riron" in *Choonpa Gijutsu Binran*, (in Japanese) edited by J. Saneyoshi, Y. Kikuchi, O. Nomoto (Nikkan Kogyo Shimbun, Tokyo, 1978), Chap. 3, pp. 381-388.
8. You-Liang Gu, "Modeling and simplification for dynamic systems with testing procedures and metric decomposition," *Decision Aiding for Complex Systems, Conference Proceedings., 1991 IEEE International Conference on Topic(s): Computing & Processing (Hardware/Software) ; Robotics & Control Systems* (10.1109/ICSMC.1991.169731), 487 - 492 vol.1 Cited by 1
9. G. S. BROSAN, "A NEW FORM OF THE TENSOR EQUATIONS OF ELECTRICAL MACHINES," Proceedings of the IEE - Part C: Monographs Volume: **107**, Issue: 12, pp. 299 – 305 (1960)
10. Shigeto Takeoka and Yoshio Yamasaki, "Acoustic Projector Using Directivity Controllable Parametric Loudspeaker Array," Proc. ICA 2010, 921, (2010)